Electronic Supplementary Material (ESI) for Lab on a Chip.
This journal is © The Royal Society of Chemistry 2020

Supplemental Information: Micro-strains in the extracellular matrix induce angiogenesis

Mary Kathryn Sewell-Loftin*[1,2,3], Joshua B. Katz[3], Steven C. George^[4], and Gregory D. Longmore^[3,5]

[1]Department of Biomedical Engineering, University of Alabama at Birmingham, Birmingham, AL 35294; [2]O'Neal Comprehensive Cancer Center, University of Alabama at Birmingham, Birmingham AL 35233; [3]Department of Internal Medicine, Washington University in St. Louis, St. Louis MO, 63130; [4]Department of Biomedical Engineering, University of California, Davis, Davis CA 95616; [5]ICCE Institute at Washington University in St. Louis, St. Louis MO 63130

^S.C. George and G.D. Longmore are Co-Senior authors of this article

*Corresponding Author:

Mary Kathryn Sewell-Loftin

Assistant Professor

Department of Biomedical Engineering

University of Alabama at Birmingham

1824 6th Avenue South

Wallace Tumor Institute, Room 630A

Birmingham, AL 35294

Telephone: (205) 934-0198

Email: mksewellloftin@uab.edu

Supplemental Figures

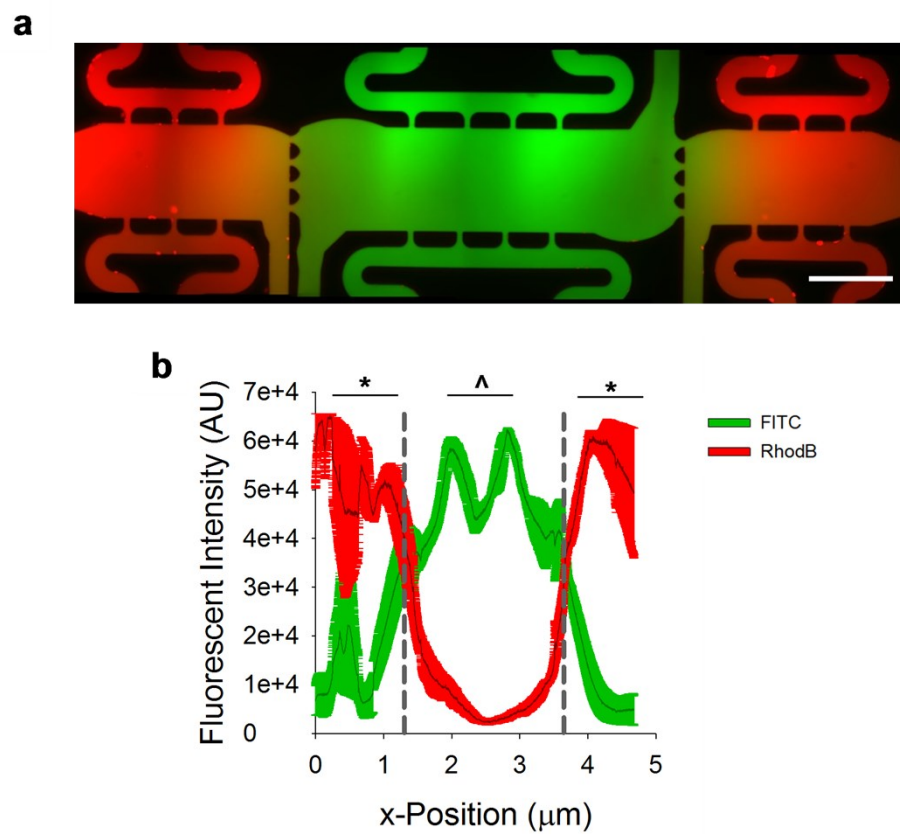

Fig. S1. Interstitial flow validation studies with low molecular weight dextrans. (a) Representative fluorescent image showing low molecular weight dextrans loaded into multi-tissue chamber devices. Center – FITC (10kDa); Sides RhodamineB (20kDa). Scale bar = 500μm. (b) Line tracings of fluorescent intensities across multi-tissue chambers loaded as described in (a). Dark line represents average intensity with ± SEM shown in the lighter color. Dashed drop lines represent tissue interfaces. Markers of significance represent comparisons between overall average fluorescent values for separate chambers. * $p < 0.01$ versus FITC intensity in center chamber; ^ $p < 0.01$ versus RhodamineB intensity in side chambers. n = three devices.

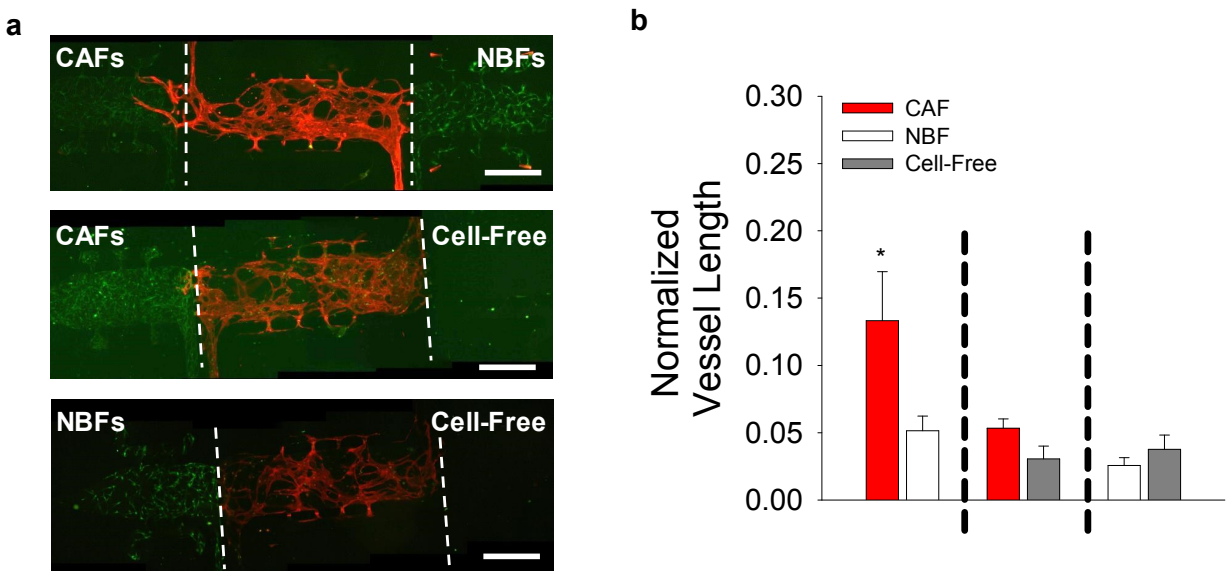

Fig. S2. Multi-tissue microfluidic device loading side chamber loading controls. (a) Representative fluorescent image of multi-tissue chamber with NHLFs and ECs in the center chamber and NBFs, CAFs, or cell-free fibrin gels in the side chambers. Devices were stained for CD31 (red) on day 8. Scale bar = 500μm. Devices were loaded with NHLFs and ECs in center chambers on day 0; side chambers were loaded with fibroblasts or blank fibrin only gels on day 4. CAFs and NBFs contain GFP. (b) Quantification of blood vessel growth into side chambers containing NBFs, CAFs, or cell-free fibrin gels * $p < 0.05$ versus NBF. n = four - eight devices, per condition.

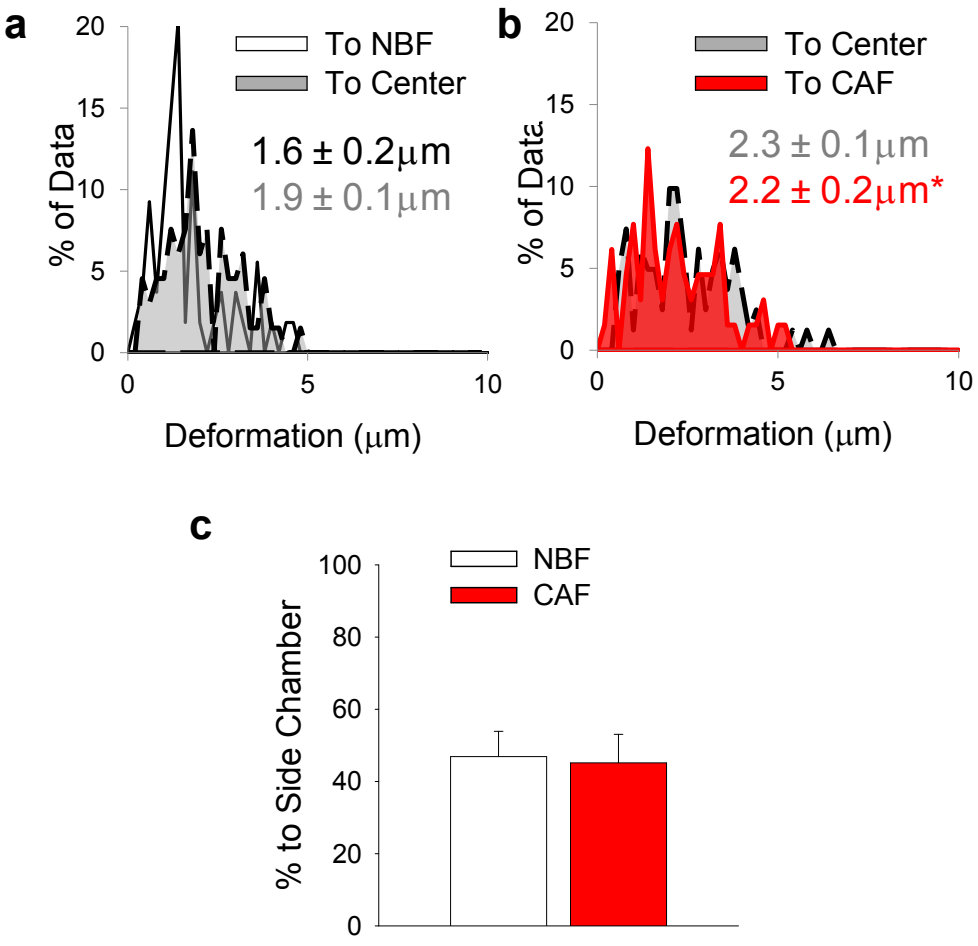

Fig. S3. Directionality of bead displacements. (a,b) Histograms showing segregated directional data for bead displacement tracking in NBF vs. CAF devices. White – To NBF chambers; Grey – To Center chambers; Red – To CAF chambers. * $p < 0.05$ vs. "To NBF" average value. (c) Quantification for segregated bead displacement directional data showing average percentage of movements towards the side chamber of each interface; a value of 50% would represent equal number of displacements tracked towards the side chamber and the center chamber at a specific interface. n = six devices.

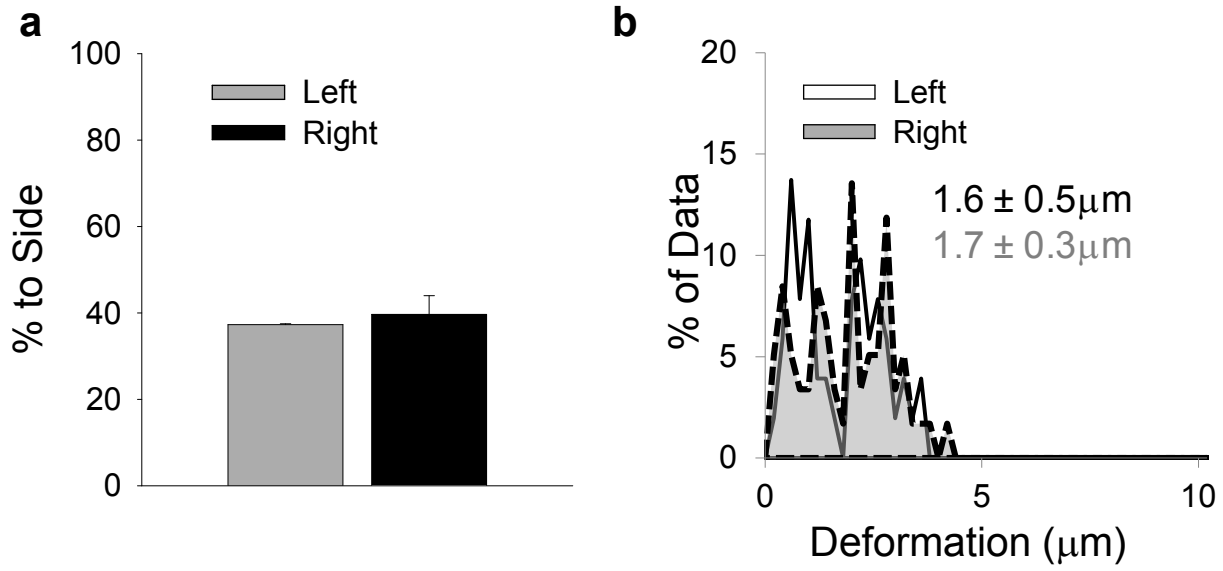

Fig. S4. Control microtissue models with cell-free side chambers. (a) Quantification for segregated bead displacement directional data showing average percentage of movements towards the side chamber of each interface for devices with NHLF/EC in the center chamber and cell-free fibrin gels in both side chambers. (b) Histogram showing deformations in ECM present in communication ports. Black/White – Interface of left and center chambers; Grey – Interface of right and center chambers. Inset numbers show average deformation magnitudes ± SEM. n = two devices.

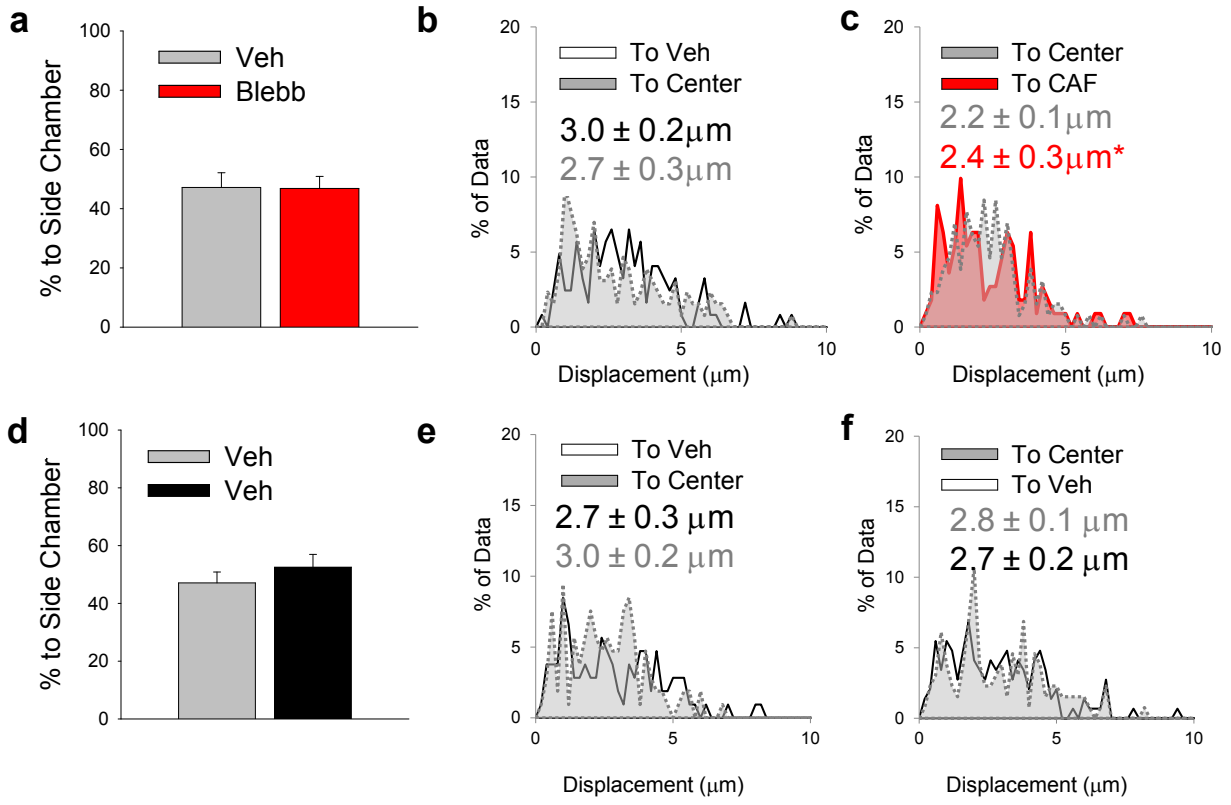

Fig. S5. Blebbistain inhibition studies effect on bead displacements in microtissues. (a) Quantification for segregated bead displacement directional data showing average percentage of movements towards the side chamber of each interface for devices treated with Veh or Blebb media. (b) Histogram showing deformations in ECM present in communication ports at interface of vehicle-treated side and center chambers. Black/White – To vehicle-treated CAFs; Grey – To Center. Inset numbers show average deformation magnitudes ± SEM. (c) Histogram showing deformations in ECM present in communication ports at interface of blebbistatin-treated side and center chambers. Grey – To Center; Red – To blebbistatin-treated CAFs. Inset numbers show average deformation magnitudes ± SEM. * $p < 0.05$ vs. “To vehicle-treated CAFs” average value. (d) Quantification for segregated bead displacement directional data

showing average percentage of movements towards the side chamber of each interface for devices treated with Veh media. (e) Histogram showing deformations in ECM present in communication ports at interface of left vehicle-treated side and center chambers. Black/White – To vehicle-treated CAFs; Grey – To Center. Inset numbers show average deformation magnitudes ± SEM. (f) Histogram showing deformations in ECM present in communication ports at interface of right vehicle-treated side and center chambers. Grey – To Center; Black/White – To vehicle-treated CAFs. Inset numbers show average deformation magnitudes ± SEM. For (a-c), n = nine devices; for (d-f) n = eight devices.

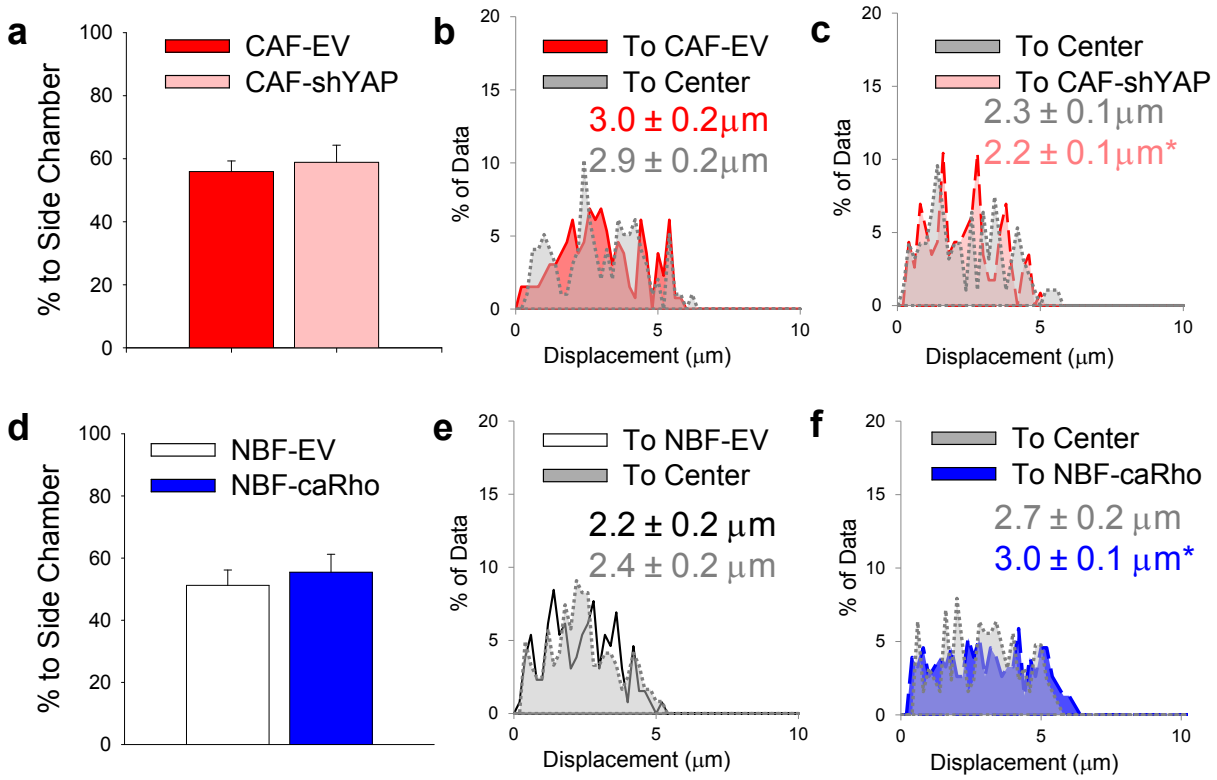

Fig. S6. Genetically-modified fibroblasts and bead displacement. (a) Quantification for segregated bead displacement directional data showing average percentage of movements towards the side chamber of each interface for devices with CAF-EV or CAF-shYAP cells. (b) Histogram showing deformations in ECM present in communication ports at interface of CAF-EV side and center chambers. Red – To CAF-EV; Grey – To Center. Inset numbers show average deformation magnitudes ± SEM. (c) Histogram showing deformations in ECM present in communication ports at interface of CAF-shYAP side and center chambers. Grey – To Center; Pink – To CAF-shYAP. Inset numbers show average deformation magnitudes ± SEM. * $p < 0.05$ vs. “To CAF-EV” average value. (d) Quantification for segregated bead displacement directional data showing average percentage of movements towards the side chamber of each interface

for devices with NBF-EV and NBF-caRho cells. (e) Histogram showing deformations in ECM present in communication ports at interface of the NBF-EV side and center chambers. Black/White – To NBF-EV; Grey – To Center. Inset numbers show average deformation magnitudes ± SEM. (f) Histogram showing deformations in ECM present in communication ports at interface of NBF-caRho side and center chambers. Grey – To Center; Blue – To NBF-EV. Inset numbers show average deformation magnitudes ± SEM. * $p < 0.05$ vs. “To NBF-EV” average value. For (a-c), n = seven devices; for (d-f), n = eight devices.

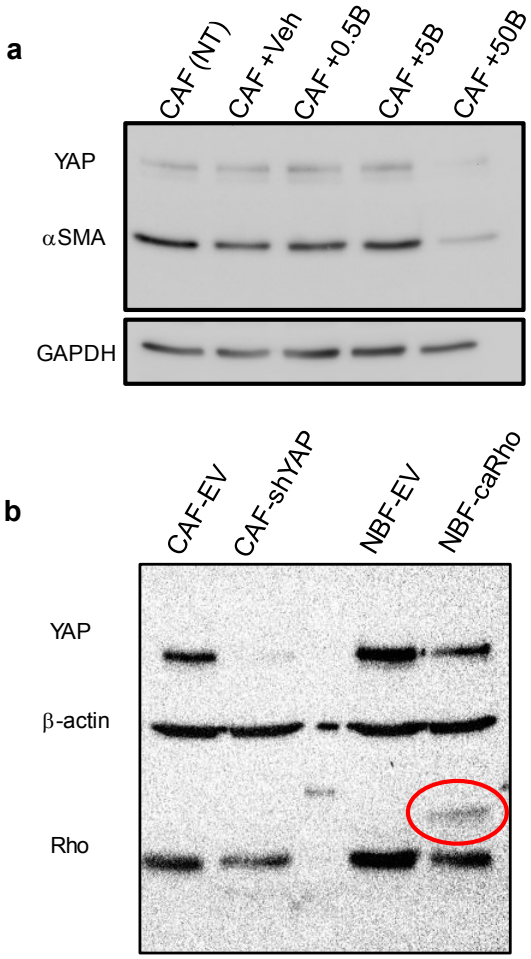

Fig. S7. Validation of stromal cell mechanotransduction markers. (a) Western blot results for CAFs showing effects of blebbistatin treatment. NT = No Treatment; Veh = vehicle. CAFs were treated with 0.5μM, 5μM, or 50μM for 24h prior to measuring protein expression of YAP and αSMA. GAPDH was utilized as the loading control. (b) Western blot results for genetically-modified stromal cells. Red circle corresponds to constitutively active Rho in NBFs (NBF-caRho) compared to NBF-EV. In these studies, β-actin was used as the loading control.

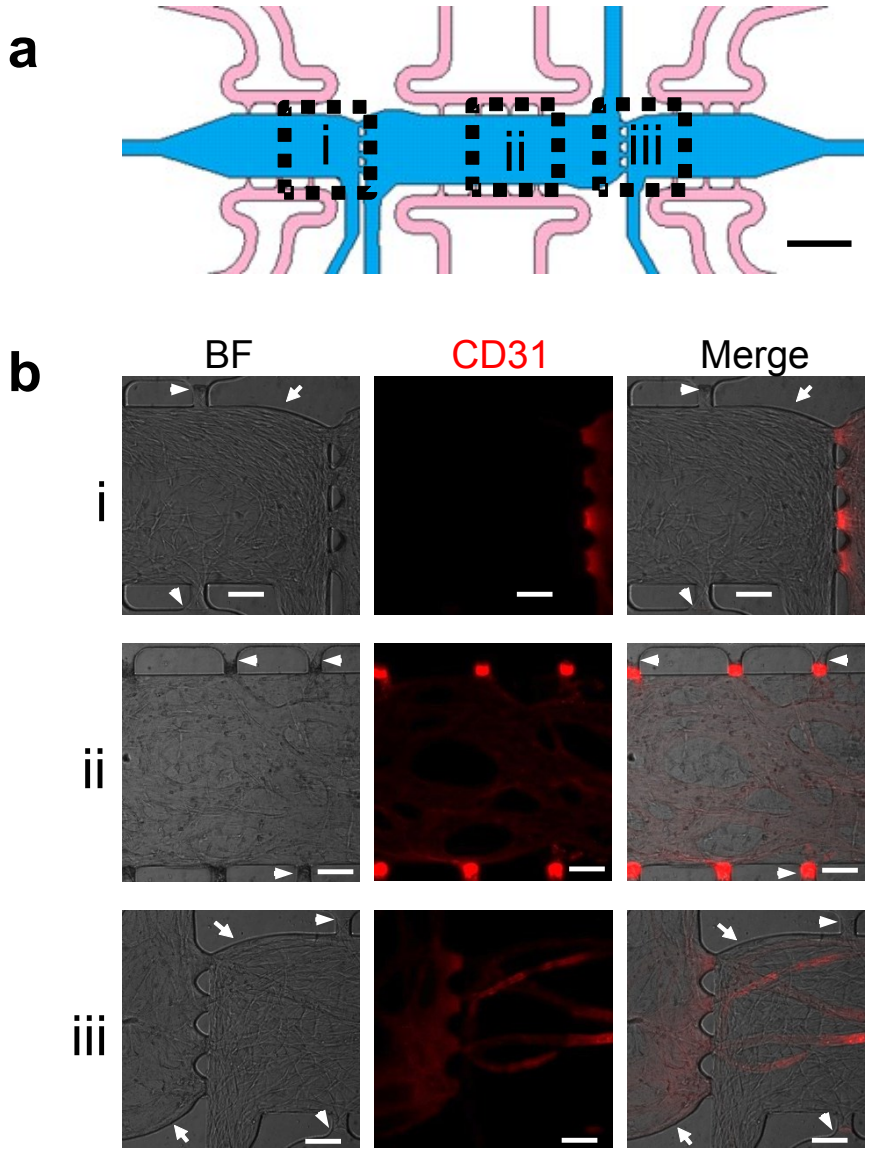

Fig. S8 – Gel integrity in microtissue models. (a) Schematic of microtissue device showing ROIs from (b). Scale bar = 500μm. (b) Representative images from microtissue devices showing that fibrin gels containing cells maintain integrity after 8 days of culture. Arrowheads correspond to edge of fibrin gel at the interface of tissue chambers and fluidic lines. Arrows highlight curved edges of side tissue chambers where no gel collapse is seen. Scale bar = 100μm. Regions i, ii, and iii correspond to inset boxes

(black dashed lines) in (a). Region i is the interface of a side chamber and center chamber, with the side chamber loaded with NBFs. Region ii is the center chamber only. Region iii is the interface of a side chamber and the center chamber, where the side chamber is loaded with CAFs. In all images, the center chambers are loaded with a 1:1 ratio of NHLFs and ECs.

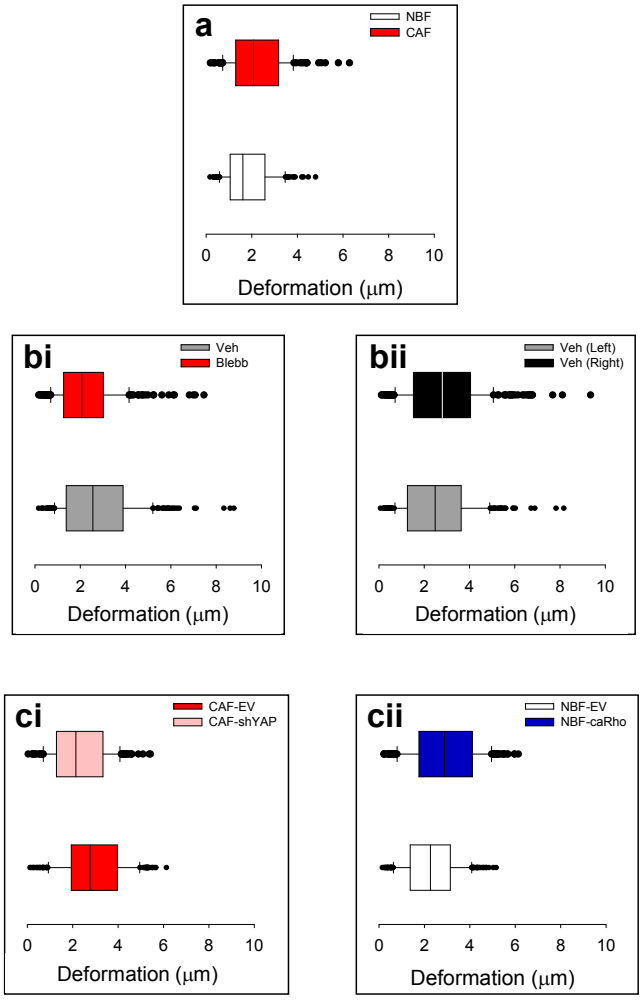

Fig. S9 – 95% Confidence intervals for bead displacements in multi-tissue devices. (a) Distribution of bead displacement magnitudes shown in Fig. 4c. (b) Distribution of bead displacement magnitudes for Fig.5c (bi) and Fig. 5f (bii). (c) Distribution of bead displacement magnitudes for Fig. 6c (ci) and Fig. 6f (cii). All distributions shown with average magnitude as drop line in center of box, with edges corresponding to 95% CI. Data points outside of 95% CI are shown as black dots. For (a), n = four devices; for (bi) n = seven devices; for (bii) n = eight devices; for (ci) n = seven devices; for (cii) n = eight devices.

Table S1. Antibodies used in Western Blots and immunoflourescent analyses

Antibody	Company	Catalog Number	Dilutions
Alexa Fluor 555 Donkey anti-Mouse	Invitrogen	A-11001	IF 1:500
Alexa Fluor 647 Goat anti-Rabbit	Invitrogen	A-32733	IF 1:500
anti-Flag tag antibody	Sigma	F3165, clone M2	WB 1:5000
Beta-actin	Sigma	T4026, clone TUB 2.1	WB 1:50000
CD31	Thermo Fisher	MA5-13188	IF 1:200
Alpha smooth muscle actin	Sigma-Aldrich	#611136	WB 1:1000
pMLC	Cell Signaling Technologies	$3671	IF 1:100
YAP	Cell Signaling Technologies	#4912	WB 1:1000